

THE FUTURE MODEL OF TA (TL)

**Shinn-Yan Lin, Hsin-Ming Peng, Weng-Hung Tseng,
Hung-Tien Lin, and Chia-Shu Liao**

**National Standard Time and Frequency Lab., TL,
Chunghwa Telecom Co. Ltd.**

**No. 12 Lane 551, Min-Tsu Rd. Sec. 5, YangMei,
TaoYuan, Taiwan 326, Republic of China
Tel: 886 3 4245483; Fax: 886 3 4245474;
E-mail: sylin@cht.com.tw**

Abstract

Telecommunication Laboratories (TL, Taiwan) published a local atomic time scale TA (TL) in November, 2004 and uses this time scale and the Circular T monthly report to calibrate a hydrogen maser/micro-phase-stepper system to be the local coordinated time scale UTC (TL). The TA (TL) is based on an ensemble of 7-9 high-performance Agilent-5071A cesium clocks. The weight of each clock was set to be proportional to the inverse exponential with the index of each clock's frequency deviation. We removed the long-term frequency drift of each clock and then weighted the residual fluctuations, in order that the frequency drift of our time scale not change too rapidly when we add or remove one clock from the ensemble. A mechanism was also developed to convert the virtual paper clock into physical output. Through this mechanism, the phase difference between the paper clock and the physical output can always be kept to within 250 picoseconds. The stability of TA (TL) is about 3×10^{-15} ($\tau = 30$ days vs. UTC); here, the average stability of the cesium clocks in ensemble is about 1×10^{-14} . We estimate this time scale to have an accuracy of 10 ns/month, and it's quite good enough to be TL's local coordinated time scale, UTC (TL).

INTRODUCTION

Telecommunication Laboratories (TL, Taiwan) participates in the formation of TAI and has disseminated UTC (TL) since 1972. We have used one cesium clock, which is steered by a micro-phase-stepper, to provide UTC (TL) from that time, and the aged model of this time scale was never changed until the end of 2004. In 2002, we began to study and try to generate our local atomic time scale. We developed a paper clock model using a cesium clock ensemble with 7-9 high-performance Agilent-5071A's. In the algorithm of this model, the weight of each clock was set to be proportional to the inverse exponential with the index of each clock's frequency deviation. Through such a weighting process, the weight of each clock will be roughly equal, which means that no clock will dominate this time scale. Meanwhile, its short-term stability is close to the traditional weighting process (inverse square of frequency deviation); only a very little worse. Another significant feature of our model is that we remove the long-term frequency offset of each clock and then weight the residual fluctuations, in order that the frequency drift of our time scale not change too rapidly when we add clocks to or remove clocks from the ensemble.

A mechanism was also developed to convert the virtual time scale into a physical output. We calculate the virtual time scale every 10 minutes and compare it to two micro-phase-steppers (each reference frequency comes from a different hydrogen maser) and adjust the frequency offset of the micro-phase-steppers if their phase output is advanced or retarded relative to the virtual paper clock. Through this mechanism, the phase difference between the paper clock and the output of the two micro-phase-steppers can always be kept to within 300 picoseconds. The stability of physical output is about 1×10^{-13} ($\tau = 600$ seconds vs. a hydrogen maser) and 3.0×10^{-15} ($\tau = 30$ days vs. UTC); here, the average stability of our clocks is about 2.5×10^{-13} and 1×10^{-14} . We estimate this time scale to have a ± 10 ns uncertainty every month, and it's quite good enough to be TL's local coordinated time scale, UTC (TL), after calibration by UTC.

THE WEIGHTING PROCESS OF THE TIME SCALE

A traditional weighting process gives the weight of each clock as being proportional to the inverse square of its frequency stability, so that one can get the most stable result for a time scale, but such a weighting process has to set an artificial upper limit; otherwise, one or a few clocks may dominate the result. We modified the traditional weighting process a little bit with inverse exponential weighting, shown below:

$$Ens(t) = TL(t) + \frac{1}{N} \sum_{i=1}^N w_i(t) \cdot [x_i(t) - (t - \Delta t) \cdot d_i(t - \Delta t)] \dots \quad (1)$$

Here, we denote $x_i(t) = UTC(TL) - clock\ i$, the phase difference between UTC (TL) and each clock; $Ens(t)$ is the UTC – ensemble clock at time t ; and $TL(t) = UTC(t) - UTC(TL)$ (t) is the phase difference between UTC and UTC (TL) at time t ; $w_i(t) = \frac{e^{-b\sigma_i^2(t-\Delta t)}}{\sum_{i=1}^N e^{-b\sigma_i^2(t-\Delta t)}}$; and $\sigma_i(t-\Delta t)$ is the Allan deviation between a hydrogen maser and *clock i* during the period $(t-\Delta t)$ to t .

The coefficient b can control the behavior of the weighting function; a large b makes the weighting function approach an inverse-square weight, and a small b makes the weighting function approach an equal weight. Here, we set the coefficient $b = 0.3 \times 10^{26}$, between an inverse square weight and an equal weight. This weighting process can filter out unreasonable or erroneous data and be only a little more unstable than the traditional weighting process in the short term. We expect the weight of each clock to approach zero when the clock is very unstable and approach an upper limit if it is very stable. We didn't set any upper limit of this weight function because the inverse exponential has an upper limit itself.

The $d_i(t-\Delta t)$ denotes the drift rate of *clock i* at the period $t - \Delta t$ to t , (compared with $Ens(t-\Delta t)$). Here, we remove the long-term frequency offset before we weight each clock, which causes the final frequency offset of the time scale to remain stable even if we remove any clock from or add any clock to the ensemble. Table 1 shows the initial file for generating the paper clock time scale. We mark the long-term frequency offset of each clock in the initial file; the time scaling procedure will remove each clock's frequency offset according to the initial file. We can also steer the frequency offset of this paper clock; changing the first row of Table 1 will adjust the frequency offset of the paper clock. We use this index to calibrate the final frequency offset.

THE FREE-RUNNING LOCAL ATOMIC TIME SCALE

The clock measurement system of TL is a system that records the phase difference between clocks, devices, and UTC (TL) (see Figure 1). A multiplexer switches the 1 PPS signal from each clock or device; a time-interval counter compares their phase with that of a hydrogen maser; and a PC workstation controls all procedures and converts the phase difference from a clock/hydrogen maser into clock/UTC (TL). Using these phase data and the weighting process discussed above, we generate a free-running local atomic time scale, TA (TL). Table 1 shows the initial file of the processing program. The left column lists the clocks in the ensemble and the right column is their long-term frequency offset; the offset is calculated by UTC – clock (i). Its value will not be changed until we remove the clock. When a new clock is added to the ensemble, we measure the frequency offset of clock during its first 6 months of stable operation, and reset the initial file. Figures 2 and 3 show the accuracy and stability of UTC – TA (TL) (MJD 52950-53300); the phase difference kept to within ± 10 ns and the 30-day stability is about 2×10^{-15} . During this period (MJD 52950-53300), we added one cesium clock, CS1012, in August 2004, and we did not find any significant change of TA (TL) around August 2004.

CONVERSION OF THE PAPER CLOCK INTO PHYSICAL OUTPUT

We also developed a mechanism to convert the time scale result into a physical output. We simulate the phase-locked loop in order to synchronize a hydrogen maser with our virtual paper clock (time scale) result. In the mechanism we developed, two micro-steppers are used for replacing the voltage control part of the phase-locked loop, and the frequency reference input of each micro-phase-stepper comes from two different hydrogen masers. Since the paper clock has no physical output, we calculate the time scale of the paper clock every 600 seconds and compare the phase difference between the paper clock and these two micro-phase-steppers at the same time.

While we treat the micro-phase-stepper as a feedback voltage control, we need a control law to adjust the frequency offset of the micro-phase-steppers. Here, we use a quasi-proportional control law to set the step of frequency-offset adjustment. That is, the more phase error the system has, the more frequency adjustment we add. To avoid having an incident phase error cause a huge frequency offset change, the control effort needs an upper limit every time we adjust the frequency offset. The upper limit should be correlated with the frequency instability between the paper clock and a hydrogen maser (about 1×10^{-13} in our measurement system). Since the phase error will not monotonically increase or decrease for a long time, it will go back and forth in a certain range; we don't need to set the upper limit to be 1×10^{-13} . We set the control effort (fractional frequency step) to be:

$$3 \cdot 10^{-14} e^{\frac{-3}{\alpha^2}} \quad (2)$$

where $\alpha = (\text{phase difference between the paper clock and the micro-phase-stepper output})/100$ picoseconds. The pattern is shown in Figure 4. If the phase error is very small, we only adjust the frequency offset by a little amount because the resolution of our measurement is just tens of picoseconds; we cannot distinguish whether it's measurement noise or not. The control effort will increase with the phase error until the upper limit 3×10^{-14} ; we expect such a control effort to compensate a larger phase

error during several frequency-offset adjustments.

Figures 5-8 show the result of this phase-locked mechanism. The phase difference between physical outputs and the paper clock can be kept to within ± 300 picoseconds over 50 days, and the two physical outputs can be kept in phase to ± 200 picoseconds. That means these two systems can closely follow the variation of the paper clock and the uncertainty is about 300 ps.

THE NEW MODEL OF TL'S TIME SCALE: TA (TL) AND UTC (TL)

Based on an Agilent-5071A cesium-clock ensemble, we generated a paper clock time scale. If the first row of the initial file (Table 1) is set to be zero, the paper clock will be a free-running time scale; we declare the free-running time scale to be our local atomic time scale, TA (TL), and have already published it in BIPM's monthly report of November 2004.

We also generated a steered time scale by changing the frequency offset of paper clock in the initial file. Here, we named the steered time scale as TATL2; it means the local atomic time scale #2. We converted the TATL2 into a physical output using the phase-locked mechanism. TATL2 can be calibrated by UTC, so that it is more accurate than TA (TL) in theory. Today, the local coordinate time scale UTC (TL) is generated from a hydrogen maser (with CAT) steered by a micro-phase-stepper; we calibrate it by UTC (on the long term) and TA (TL) (on the short term). We expect TATL2 and its physical output to be used as UTC (TL) in the near future.

CONCLUSION

TL has kept and disseminated the national standard time and frequency of Taiwan for a long time. Before 2002, we used only one cesium clock steered by UTC to be UTC (TL). The phase difference between UTC and UTC (TL) had a large phase difference, from -200 ns to +500 ns. After 2002, we began to study the behavior of each clock and tried to develop our own time scale algorithm, choosing the most stable cesium clock and paying attention to adjustment of the frequency offset at all times. The effect was that UTC – UTC (TL) was kept to within ± 100 ns after 2002. Figures 9 and 10 show the improvement of TL after 2002. Figures 10 and 11 also show the accuracy and stability of TA (TL); the 30-day stability can reach 2×10^{-15} . The TATL2 will be more accurate than TA (TL) in theory, but generating the physical output of TATL2 needs more procedures than our old model; any mistake in those procedures will cause system damage. We have to be very careful before we define TATL2 as UTC (TL).

REFERENCES

- [1] D. W. Allan, 1987, "Time and frequency (time domain) characterization, estimation, and prediction of precision clocks and oscillators," **IEEE Transactions on Ultrasonics, Ferroelectrics, and Frequency Control**, UFFC-34, 647-654.
- [2] **Handbook Selection and Use of a Precise Frequency and Time System** (ITU, 1997), Chapter 6.

- [3] J. Azoubib, M. Granveaud, and B. Guinot, 1977, “*Estimation of the scale unit duration of time scales,*” **Metrologia**, **13**, 87-93.
- [4] P. Tavella and C. Thomas, 1991, “*Comparative study of time scale algorithms,*” **Metrologia**, **28**, 57-63.
- [5] S. Lin and H. Peng, 2004, “*A paper clock model for the cesium clock ensemble of TL,*” in Proceedings of the 35th Annual Precise Time and Time Interval (PTTI) Systems and Applications Meeting, 2-4 December 2003, San Diego, California, USA (U.S. Naval Observatory, Washington, D.C.), pp. 297-306.
- [6] S. Lin, 2004, “*A Phase Locked Mechanism for Time Scaling Frequency Control System,*” in Proceedings of the 2004 IEEE International Ultrasonics, Ferroelectrics, and Frequency Control Joint 50th Anniversary Conference, 24-27 August 2004, Montreal, Canada, in press.

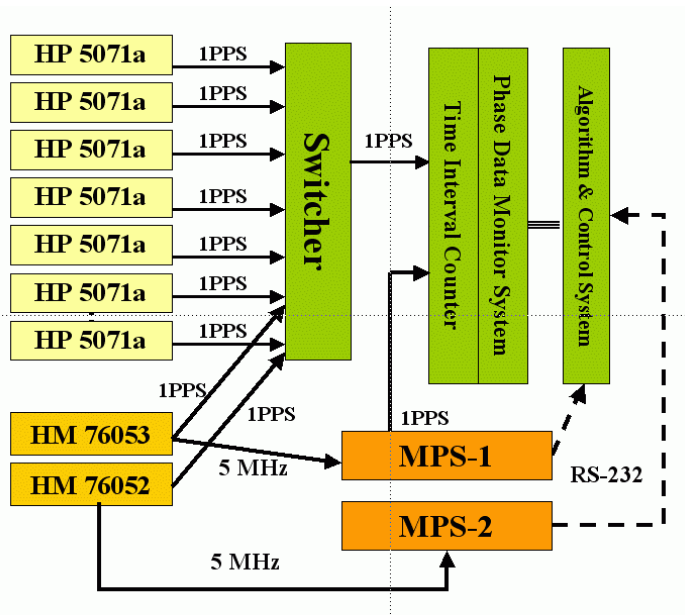


Figure 1. System architecture, including seven cesium clocks, two hydrogen masers, two micro-phase-steppers, one time-interval counter, and the controlling computer server.

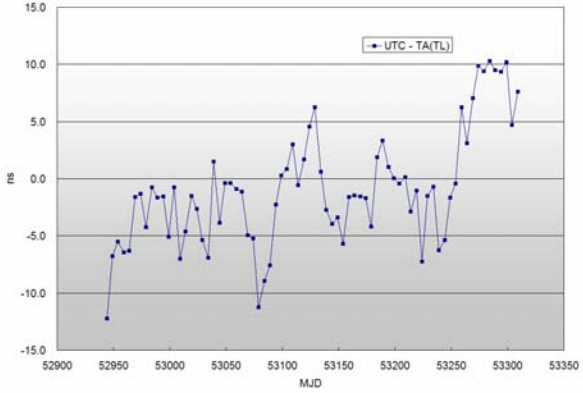


Figure 2. Phase difference between UTC and TA (TL).

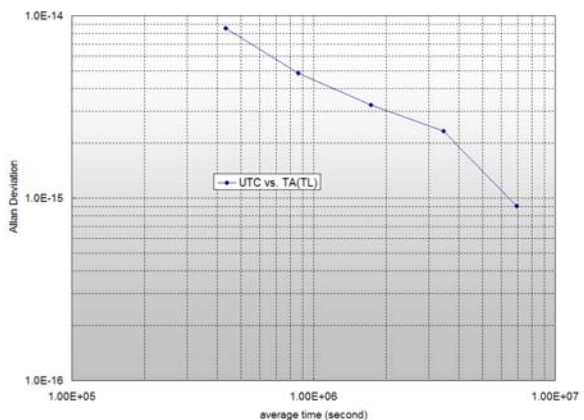


Figure 3. The stability of UTC – TA (TL).

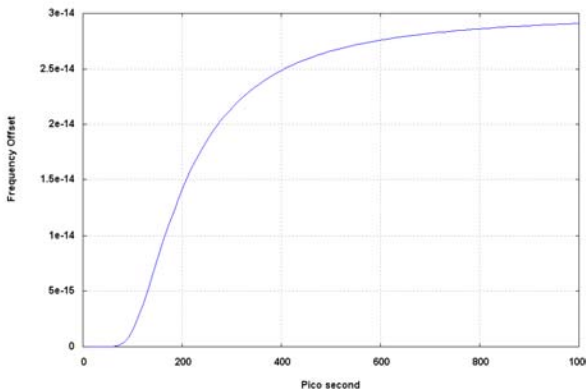


Figure 4. The pattern of control law:
 $3 \times 10^{-14} \cdot \exp(-3/(\alpha^* \cdot 2))$.

TATL1	-0.00000
HM6053	-1.79200
CS0160	-7.36680
CS0300	+8.15348
CS0474	+21.95141
CS0809	+2.14309
CS1012	+6.80201
CS1132	-3.31303
CS1498	+14.72922
CS1712	+0.52046

Table 1. The initial file for generating the time scale TA (TL), units in ns/day.

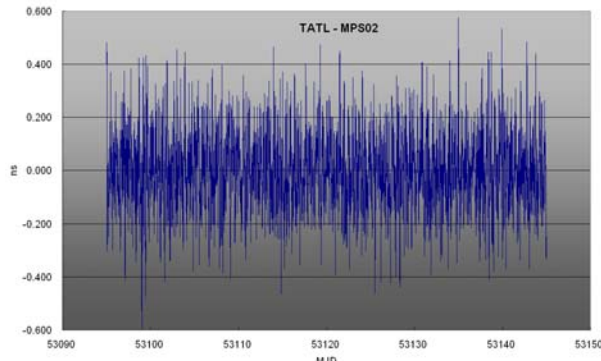


Figure 5. The phase difference between the output of micro-phase-stepper #2 and TA (TL).

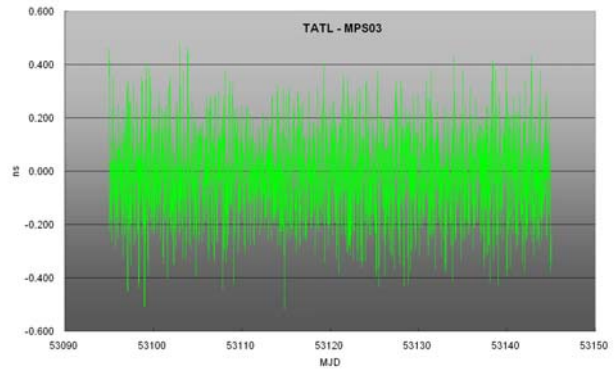


Figure 6. The phase difference between the output of micro-phase-stepper #3 and TA (TL).

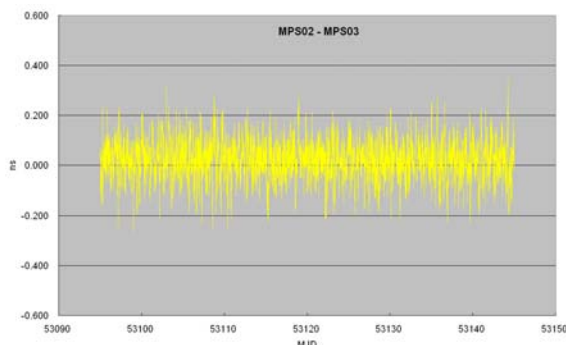


Figure 7. The phase difference between the outputs of micro-phase-stepper #2 and #3.

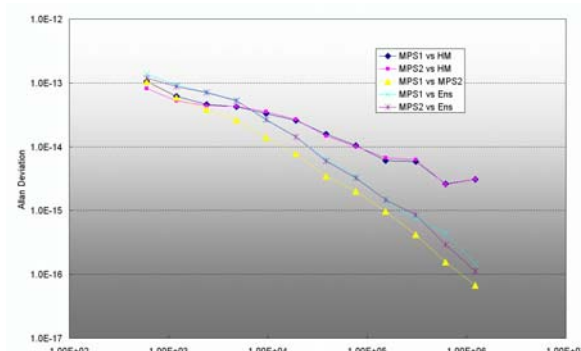


Figure 8. The stability between the output of the micro-phase-steppers, a hydrogen maser, and the paper clock.

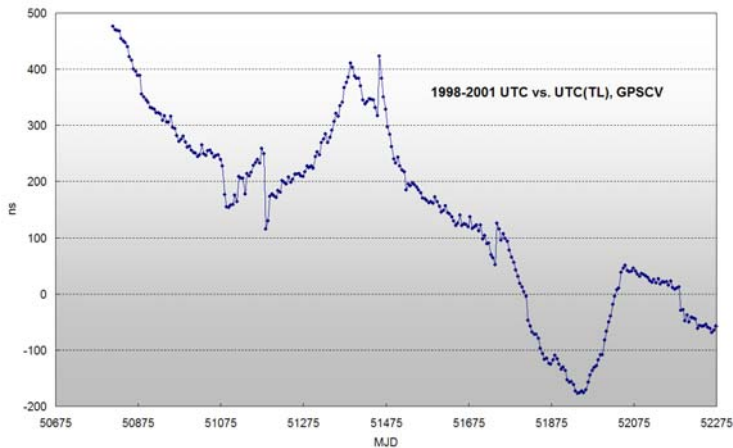


Figure 9. UTC – TA (TL), before 2002.

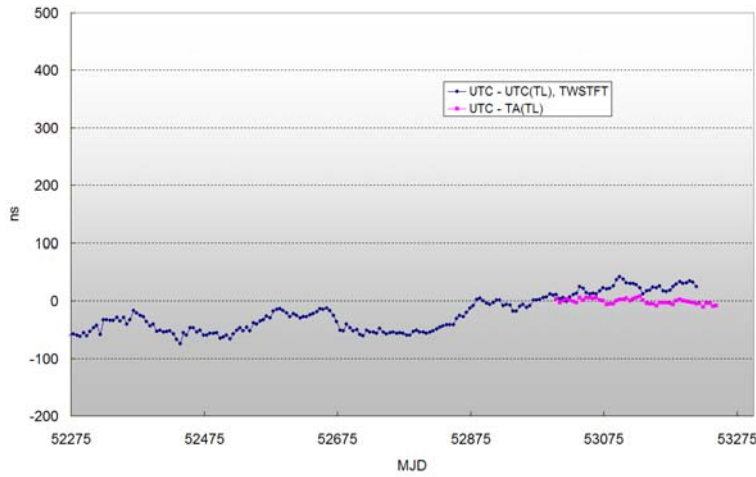


Figure 10. UTC – UTC (TL) and TA (TL), from 2002 to October 2004.

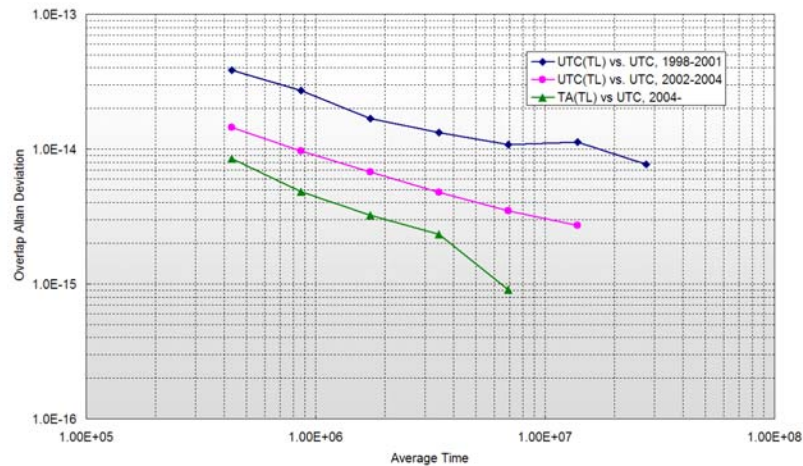


Figure 11. The Allan deviation of UTC – UTC (TL) and UTC – TA (TL).